Investigation of the optical-absorption bands of Nb^{4+} and Ti^{3+} in lithium niobate using magnetic circular dichroism and optically detected magnetic-resonance techniques

H.-J. Reyher, R. Schulz, and O. Thiemann
Universität Osnabrück, Fachbereich Physik, D-49069 Osnabrück, Germany
(Received 29 October 1993; revised manuscript received 29 March 1994)

The magnetic circular dichroism (MCD) of the absorption of Nb_{Li}^{4+} and Ti_{Li}^{3+} centers in $LiNbO_3$ has been selectively measured by applying optically detected magnetic resonance. The attribution of a well known broad and unstructured absorption band peaking at 1.6 eV to the Nb_{Li}^{4+} bound small polaron is now unambiguously confirmed. In the MCD spectrum of the isoelectronic Ti_{Li}^{3+} center, bands show up, which closely resemble the MCD bands at 1.6 eV of this bound small polaron. This striking similarity is explained by a cluster model, representing both defects. Either Ti_{Li} or Nb_{Li} is at the center of this cluster. In both cases, the small polaron is bound to the cluster, and its MCD bands correspond to intervalence transfer transitions within the constituents of the cluster. A study of the spin-orbit coupling of the molecular orbitals of the cluster allows one to analyze the structure of the MCD bands connected with these transitions. Well-structured MCD bands at 2.9 eV of Ti_{Li}^{3+} have no counterpart in the Nb_{Li}^{4+} spectrum. These bands are assigned to transitions to excited states, which are specific to the impurity and are related to the $10Dq$ transitions known for the crystal field states of a d^1 ion.

I. INTRODUCTION

From the very beginning of the research on lithium niobate numerous contributions appeared in the literature concerning the optical bands originating from transition metal impurities.[1,2] The continuing interest in this topic results from the aim to reveal the basic mechanisms underlying the photorefractive and photovoltaic properties of this material.[3,4] A most valuable help for the interpretation of the photorefractive dynamics and related problems[5] would consist in an unambiguous correlation between the defects and the absorption bands caused by them, but "all interpretations of the spectra suffer from the broad absorption bands observed and from the overlapping of spectra from ions in different charge states."[1] Consequently, attempts have been made to decompose the spectra into several components, which then have been attributed to certain defects. This has been done by reduction and thermal bleaching experiments for both pure and doped $LiNbO_3$.[6] Especially, the contribution to the absorption from the intrinsic defect consisting of a Nb^{4+} ion on a Li site could be examined in a more specific way, since its electron-paramagnetic-resonance (EPR) spectrum has been identified in both irradiated[7] and reduced undoped $LiNbO_3$.[8] Correlating the optical absorption with the EPR line intensity[7,9,10] led to the attribution of a broad, asymmetric band peaked at about 1.6 eV to the Nb_{Li}^{4+} bound small polaron.

Although the mentioned experiments yielded important information, we have to point out that any attribution given so far is based on only indirect conclusions. A simultaneous change in signal intensity of both absorption and EPR, due to some treatment, does not *necessarily* mean that both observables result from the same defect. In order to correlate EPR with optical absorption in a more direct way, we have measured the magnetic circular dichroism (MCD) of the absorption spectra resulting from Nb_{Li}^{4+} in $LiNbO_3$. As discussed briefly below, the MCD may be "tagged" to the underlying defect by electron spin resonance, which in this case is called optically detected magnetic resonance (ODMR). By this method, the "EPR fingerprint" is transferred to optical spectra. Furthermore, MCD bands usually provide additional information on the nature and the composition of the observed spectra in comparison with simple absorption measurements. As a consequence, studies of "tagged MCD" spectra allow both to separate bands of one defect from those of another and to attack the intriguing problem concerning the nature and symmetry of the excited states involved in the absorption process. Although, in general, MCD spectroscopy exceeds ordinary absorption measurements by increased spectral resolution, the bands observed in the case of Nb_{Li}^{4+} in $LiNbO_3$ turned out be very broad and to overlap considerably. Therefore, comparative studies of the isoelectronic ion Ti_{Li}^{3+} in $LiNbO_3$ have also been performed.[11]

II. EXPERIMENTAL METHODS

The MCD is defined to be the difference of the absorption coefficients for left and right hand polarized light induced by a magnetic field. As is well known in MCD spectroscopy,[12–14] there exists a paramagnetic contribution to the MCD for paramagnetic impurity centers in crystals, which predominates over other, diamagnetic parts at low temperatures, if the absorption bands are broad. This condition is very well fulfilled in our case.

 ©1994 The American Physical Society

To a good approximation, the bands forming the paramagnetic MCD spectra possess the same shape as those observed in usual zero field absorption measurements. The relative amplitudes, however, need not be the same and both signs are possible for MCD bands. For systems with spin $S = 1/2$, like Ti^{3+} or Nb^{4+}, one can show,[12] that the paramagnetic part of the MCD is proportional to the spin polarization of the ground state. Due to this fact the spin resonance, affecting this polarization, may be observed optically (ODMR) as a change (usually a decrease) of the MCD signal. It follows that the amplitude of the ODMR signal yields a measure of that fraction of the MCD, which originates from the center being at resonance. This explains why a spectrum consisting of the ODMR intensity as a function of photon energy has been called the "tagged MCD" spectrum.[15]

The selectivity of the method clearly depends on the existence of an unambiguous ODMR signal; i.e., special care has to be taken if ODMR lines of several defects overlap, as is the case for Ti^{3+} and Nb^{4+}. Moreover, situations have been encountered,[16] in which ODMR signals from one center could be observed via the MCD of another impurity, *although* the resonance lines were well separated. In view of this, a thorough examination of the conventional EPR and ODMR spectra has been performed using samples with different ratios of defect concentrations.

The most relevant properties of the crystals used are listed in Table I. All specimens were prepared from congruent $LiNbO_3$ and have been chemically reduced by some treatment mentioned in the table in order to obtain the paramagnetic charge states Ti^{3+} and Nb^{4+}.

Our experimental setup consists of an optical helium cryostat with a 3 T superconducting magnet. Measurements are typically performed at 2 K. The MCD signal is measured dynamically using the lock-in technique and an elasto-optical modulator, which switches between left and right circularly polarized light at a rate of 40 kHz. As only broadbands are observed, we limit the spectral resolution of the light source (lamp and monochromator) to about 3 nm. Magnetic resonance may be performed at microwave frequencies of 35 GHz (klystron) and 70 GHz (Gunn diode). No cavity is used, the crystals simply being fixed below the end of the waveguide leading into the cryostat.

The sign of the experimental MCD has been checked by a $\frac{\lambda}{4}$ plate (with known direction of the slow axis) in combination with a polarizer acting as an absorber for left circular light. A compass was used to determine the direction of the magnetic field. This check was further confirmed by the observation of the MCD of $Bi_{12}GeO_{20}$ at about 600 nm, which is characteristic for all crystals of this type and which we found to be negative in accordance with the measurements of Briat *et al.*[17] Briat *et al.* have checked their apparatus by a number of substances with known sign, including F centers in alkali halides. In the following, the sign of the MCD is according to the standard definition MCD$\propto \alpha_+ - \alpha_-$, where $\alpha_{+/-}$ are the absorption coefficients for left and right circular light, respectively.[12–14]

III. RESULTS

A. EPR and ODMR

In sample 1 only the (conventional) EPR and the ODMR lines of Ti^{3+} could be detected. Since Nb^{4+} shows a very characteristic resonance spectrum (Fig. 1), it can be concluded that with this crystal only MCD bands tagged to Ti^{3+} will be obtained.

Crystal 2 is a typical representative of intentionally undoped, reduced $LiNbO_3$ crystals examined in our group: The EPR lines of both Ti^{3+} and Nb^{4+} can be seen simultaneously at low temperatures and after illumination with visible light. Light irradiation results in an increase of the Nb^{4+} signal, while the Ti^{3+} line decreases to some extent.[9] Typical spectra obtained at 34 GHz are shown in Fig. 1. Since light illumination is inherently connected with the ODMR method, both types of centers might be expected to contribute to ODMR signals of crystal 2.

Finally, sample 3 exhibits a strong EPR signal due to Nb^{4+} even before illumination. A possible contribution from Ti^{3+} could not be resolved in conventional EPR, because the Nb^{4+} pattern is rather complicated[18] and a unique decomposition of the observed spectrum is not possible for low Ti concentrations [Ti]. In any case, however, the ratio $[Ti^{3+}]/[Nb^{4+}]$ is much smaller in sample 3 than in specimen 2. No further paramagnetic centers could be detected in all three samples by EPR.

Figure 2 shows an ODMR spectrum of crystal 2 obtained at 70 GHz. Within the experimental error, the g value and the total width agree with the data of Nb^{4+} from conventional EPR. As often observed, the hyperfine structure is not resolved in ODMR in contrast with EPR (Fig. 1). To our knowledge, the reason for the differ-

TABLE I. Sample properties. The last column indicates the EPR-line intensity for the corresponding center.

Sample	Doping	Reduction treatment	Source	EPR lines
1	Ti, 1.4 mol.% in the crystal	27 h, 900 K, in vacuum, in Li_2CO_3 powder	central research laboratories Siemens AG München	Ti^{3+} only
2	nominally undoped	6 h, 1370 K, in vacuum	Institut für Angewandte Festkörperphysik, Freiburg	Ti^{3+} and Nb^{4+}
3	nominally undoped	2 h, 1270 K, in vacuum	central research laboratories Siemens AG München	$Nb^{4+} \gg Ti^{3+}$

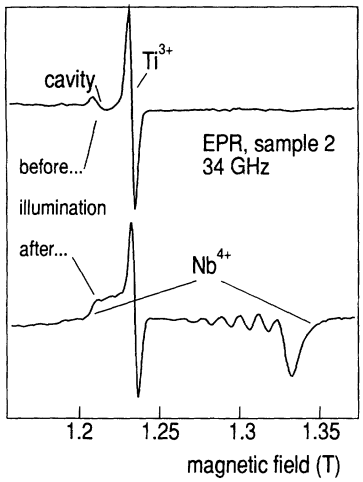

FIG. 1. EPR of sample 2 containing both Ti^{3+} and Nb^{4+} centers. The signal marked by "cavity" arises from some paramagnetic perturbation in the microwave cavity.

ent resolution of the two methods is not yet understood. However, the most important fact for the subsequent argumentation consists in the lack of a Ti^{3+} related signal, which should be positioned near the thick arrow in Fig. 2. Consequently, the sensitivity of ODMR is considerably lower than that of conventional EPR in the case of Ti in $LiNbO_3$. In comparison with sample 2, crystal 3 shows an ODMR line of similar strength and practically identical shape. As the latter specimen was characterized by EPR to have a much lower ratio $[Ti^{3+}]/[Nb^{4+}]$, it is not surprising that Ti is absent in the ODMR spectrum of sample 3, too. Hence, all these observations lead to the statement that tagged MCD spectra obtained from sample 2 or 3 must be attributed exclusively to Nb^{4+}.

At 35 GHz, where all tagged MCD measurements have been performed because of experimental reasons, the resonances of both defects do overlap. However, it is plausible to assume that the relative sensitivities for Ti and Nb are left unchanged at 35 GHz with respect to 70 GHz.

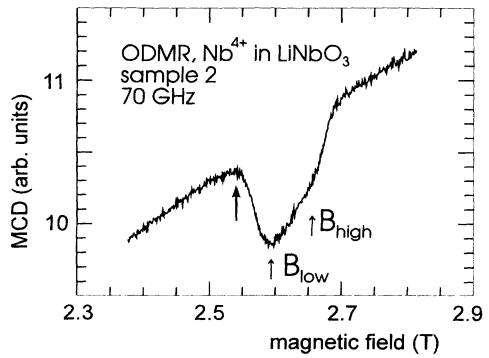

FIG. 2. ODMR of the Nb^{4+} small polaron in $LiNbO_3$ at 70 GHz. The thick arrow marks the position, where the resonance of Ti^{3+} is expected. B_{high} and B_{low} correspond to positions within the ODMR line, where the tagged MCD spectra have been measured at 35 GHz (see end of Sec. III B).

Furthermore, as for 70 GHz, the ODMR spectra are identical for specimens 2 and 3. Again, this finding could not be understood if Ti^{3+} would contribute significantly to the observed ODMR lines. In summary, we conclude that the MCD spectra to be presented in the following section are selectively tagged to either niobium (sample 2 and 3) or titanium (sample 1).

B. Tagged MCD and absorption spectra

Parts (a) and (b) of Fig. 3 show the MCD spectra tagged to Nb^{4+} and Ti^{3+}, respectively. The corresponding absorption curves, to be discussed later, are depicted below in parts (α) and (β) to allow convenient comparison.

Before discussing the possible nature of the observed bands, we want to report some further experimental tests, which show that the MCD bands presented above are really selective. This is even more important, because the striking similarity of the two oppositely directed bands below 2.2 eV in Figs. 3(a) and 3(b) might still be suggested to result from cross-talk effects.

According to the definition of the tagged MCD, the ordinate in Fig. 3(a) represents the amplitude of the ODMR signal (in arbitrary units) of Nb^{4+}. The depicted spectrum has been taken with the magnetic field at some value B_{low} in the lower part of the ODMR line, where also the Ti resonance is located at 35 GHz [compare Figs. 1 and 2 (Ref. 19)]. At B_{high}, in the upper regime of the ODMR curve, an identical shape of the tagged MCD is detected. If the ODMR signal would contain a substantial contribution from Ti^{3+}, this fraction, being different for B_{low} and B_{high}, would lead to different MCD spectra when tagged at these two magnetic fields. Suffice to say that also both the MCD spectra for sample 2 and 3, containing a different amount of Ti, are the same. We therefore definitely exclude that an artifact is at the origin of the similarity of the low energetic MCD bands of Ti^{3+} and Nb^{4+} in $LiNbO_3$ and will interpret this feature in the next section by a physical model.

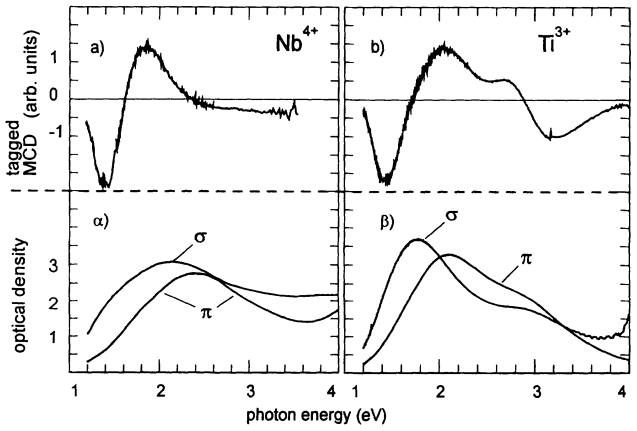

FIG. 3. Tagged MCD spectra of (a) $LiNbO_3$:Nb^{4+} and (b) $LiNbO_3$:Ti^{3+} at 35 GHz. The lower parts (α) and (β) show the corresponding absorption spectra for σ and π light.

IV. DISCUSSION

In the following sections we will first construct a model representing the investigated isoelectronic centers. From this model we then decide upon the MCD bands to be expected. By comparison with the experimental spectra, we finally arrive at an interpretation of the observed MCD bands. In particular, this interpretation accounts for the structure of the MCD observed at low energies, common to both defect ions. In the case of Nb_{Li}^{4+}, the corresponding absorption band at 1.6 eV is identical to the bound small polaron band of Ref. 2. Polaronic or relaxation related aspects are not considered in this paper.

A. Defect model

A calculation of MCD bands requires in principle the knowledge of the structure of the initial and final states taking part in the optical transitions. In the present case, the ground state is rather well known from EPR analysis for both ions.[18,20] It may be described by a crystal-field state transforming according to the representation A_1 of the group C_{3v}. For ease of further argumentation the level splitting diagram for a d^1 system in the sequence of decreasing strength of interaction (cubic crystal field, trigonal field, and spin-orbit coupling) is shown in Fig. 4. Such a scheme is known to be useful for a characterization of optical bands as long as the involved states are within the band gap and are localized predominantly at the impurity ion. However, the energetic position of the $Nb^{4+/5+}$ level was determined by conductivity and thermopower measurements to be only about 0.4 eV below the conduction band.[21] The $Ti^{3+/4+}$ level, on the other hand, is placed about 0.1 eV below $Nb^{4+/5+}$ according to thermal activation studies of EPR signals.[20] Consequently, all the observed MCD bands, being located above 1 eV, correspond to transitions, whose final states are energetically degenerate with conduction band states or simply are of that type. That is, a description in terms of crystal-field states becomes doubtful.

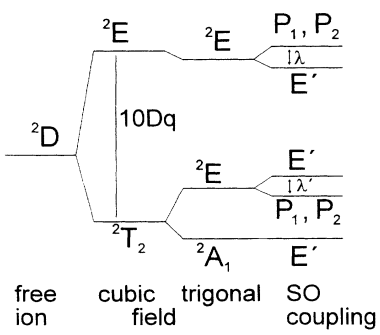

FIG. 4. Level scheme of a d^1 ion in a cubic, trigonal crystal field and under the influence of spin-orbit coupling. The labels indicate the irreducible representations of the states (according to Ref. 14). The spin-orbit splitting λ of the E state at $10Dq$ is zero to first order. The ratio of $10Dq$ to the trigonal splitting of the T_2 state is typically 20–30 (Ref. 20).

The example of the As_{Ga} antisite in GaAs (Ref. 22) shows that the MCD line shape can be calculated for a transition from a localized state to band states almost from first principles, if the band structure is known. Unfortunately, this is not the case for $LiNbO_3$ and a different description of the excited states has therefore been chosen: Symmetry-adapted molecular orbitals (MO's) of the linear combination of atomic orbitals (LCAO) type are constructed using ground state atomic orbitals $|dt_2a_1\rangle$ located at the central impurity ion and the *next-nearest* niobium neighbors (NNN's). The atomic orbitals (AO's) are labeled in a "chain" notation (free ion, cubic, trigonal representation),[14] whose meaning becomes clear from Fig. 4. The limitation on the region enclosed by the NNN means that the molecular states, considered here, are much more localized than the Bloch states used in the case of GaAs. This assumption may be justified by the "more ionic" character of $LiNbO_3$. There is also another argument why the applied method should be appropriate to describe intervalence transfer transitions from the deep impurity level to the Nb ions of the host lattice: In some sense, it represents an adoption of the methods used in such MCD studies, where the AO's of the *nearest* neighbors, i. e., the ligands, are considered. Corresponding calculations have been successfully used to explain MCD spectra of charge transfer transitions,[14] where the optical excitation transfers electrons or holes between ligandlike and impuritylike states. Most recently, the MO approach has been applied successfully to the MCD spectrum of the Zn vacancy V_{Zn} in ZnSe.[23] There, the relevant MO states are built from hole type AO's entirely localized on the four Se atoms surrounding the vacancy. As this study is closely related to the present work, we will discuss the similarities and differences in more detail in Sec. V.

The construction of MO's from AO's $|dt_2a_1\rangle$ alone is a very crude approach. Especially, it will be shown in the Appendix that the restriction on AO's of that type necessarily leads to zero spin-orbit coupling in any of the resulting MO's. The simple AO basis used below is therefore actually not sufficient to describe MCD properties. Nevertheless, even in the rudimentary present form the model will well be able to show what will happen if also $|dt_2e\rangle$ AO's (see Fig. 4) will be included in a more elaborate work. This point and also the neglect of the excited $|dee\rangle$ states will be discussed below. This will be done more easily after presenting the results of a model calculation including only the $|dt_2a_1\rangle$ states.

Figure 5 shows the cluster of ions which are considered in the model calculation. The central ion 0, either Nb^{4+} or Ti^{3+}, is placed on a Li site, in accordance with shell model calculations[24] and extended x-ray-absorption fine-structure (EXAFS) measurements,[25] respectively.

The next-nearest Nb_{Nb} ions 1–6 are shown as well as those oxygen ions forming bonds between them. Because the six Nb_{Nb} ions reside on the corners of two triangles, rotated against each other by 60°, the point symmetry of the cluster is C_{3v}. A slight distortion of the oxygen triangles,[1] leading to C_3, is ignored.

Except for the central one, there are no lithium positions inside the cluster. The AO's $|i\rangle$ of type $|dt_2a_1\rangle$ are located on the metal constituents, numbered by i in

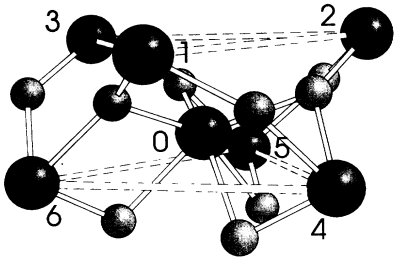

FIG. 5. Fragment of $LiNbO_3$ consisting of a central ion 0 (Ti^{3+} or Nb^{4+}) on a Li site and the next-nearest Nb_{Nb} ions (1–6). The oxygen ions forming bonds between the cations are shown with a lighter texture. The dashed sticks have been added to illustrate the trianglelike symmetry of the cluster. If ion 0 is ignored, ions 1–6 form a molecule, which has similar symmetry properties as benzene.

Fig. 5, and are coupled via the matrix elements of an appropriate Hamiltonian h, $\langle i|h|j\rangle = h_{ij}$. Dealing with a model calculation to describe the qualitative features of the MCD, we do not investigate the nature of h or want to give quantitative estimates for the values of the particular h_{ij}, which are also determined by oxygen states acting as "intermediaries."[26] The Hamiltonian matrix h_{ij} was chosen as follows:

0	1	2	3	4	5	6	
0	K	K	K	L	L	L	0
	ϵ	0	0	$-J$	0	$-J$	1
		ϵ	0	$-J$	$-J$	0	2
			ϵ	0	$-J$	$-J$	3
	c.c.			ϵ	0	0	4
					ϵ	0	5
						ϵ	6

Values for the parameters J, K, and L, representing the off-diagonal elements, have been chosen in the sequence $J = K < L$, according to the number of oxygen bridges between the respective Nb ions. Matrix elements, which account for coupling via more than one intermediary, are simply set to zero. Those between ions of the two Nb triangles read as $-J$, because with that sign a benzenelike sequence of states is obtained,[27] if ion 0 is omitted. In this case one may formally set $K = L = 0$ in the Hamiltonian and both Nb triangles become equivalent. The cluster then topologically corresponds to the benzene molecule.

The diagonal matrix elements ϵ were chosen to be much larger than L, since they account for the energy difference between placing an electron on Nb_{Nb} rather than on Nb_{Li} (or Ti_{Li}) in the fully localized limit, i.e., when J, K, and L are neglected. That is, ϵ roughly describes the position of the Nb^{4+}_{Li} level (or Ti^{3+}_{Li} level) relative to Nb_{Nb} states, which form the conduction band, if the whole crystal is considered. The off-diagonal elements J determine the splitting within the Nb_{Nb}-related or conduction-band-like states, while K and L cause mutual admixtures of Nb_{Nb} and Nb_{Li} or Ti_{Li} orbitals to ground and excited states, respectively. It should be pointed out that ϵ must be larger than the value of 0.4 eV obtained from conductivity and thermopower measurements[21] (see above). The latter experiments use *thermal* instead of optical excitation of the electron to conduction-band-like states. Optical transitions occur to excited Nb_{Nb} states before lattice relaxation, whereas the thermal activation is via Nb_{Nb} orbitals imbedded in a somewhat relaxed surrounding.[28] In contrast with Ref. 23 nearest-neighbor states are not included in the basis, because hole states are not involved in the transitions considered here. Covalency with oxygen is neglected as the corresponding valence-band-like states are too low in energy.

We investigate the properties of the MO's of the cluster according to the general procedures outlined in Ref. 26: The eigenvalues and eigenvectors of the above matrix are calculated numerically for convenient values of the parameters. Inspection of the symmetry of the eigenvectors shows that two E states result and four states of type A_1, one of which being the ground state with predominant Nb_{Li} or Ti_{Li} character, i.e., containing a large fraction of state $|0\rangle$. However, one must point out that this state still has nonzero admixtures (of the order $\frac{K}{\epsilon}$) of orbitals $|i \neq 0\rangle$. These admixtures will become relevant below, when the intensity of the transitions will be considered. The specific values used for the matrix elements need no further discussion, since we want to restrict the discussion on those features of the results which only weakly depend on that particular choice. Also, only excited states of symmetry E will be considered because of the selection rules appropriate for MCD measurements (see the next section).

The energy of these excited E states does not depend on K or L, and the corresponding eigenvectors do not contain the orbital of the central ion $|i = 0\rangle$. This result clearly originates from the symmetry of the AO's used as a basis, because a molecular state of symmetry E must not have an atomic orbital $|dt_2a_1\rangle$ at the center of symmetry. This is no longer valid if the $|dt_2e\rangle$ orbitals (Fig. 5) of the central ion, $|i = 0\rangle_e$, are added to the basis. However, the admixture of the orbitals $|i = 0\rangle_e$ to the excited molecular state $|E\rangle$ will be of the order $\frac{h_{ij}}{\epsilon}$, which is assumed to be a small number. Also, the AO's of type $|dt_2e\rangle$ located at Nb_{Nb}, $|i \neq 0\rangle_e$, should be included into the basis in a more realistic model. These states are energetically close to $|i \neq 0\rangle_{a_1}$ with energies $h_{ij} \approx \epsilon$, and thus must not be regarded as small admixtures. A full incorporation of these states $|i \neq 0\rangle_e$ is beyond the scope of this paper. However, from the comparison with the similar case of benzene, it is clear that additional excited molecular states transforming as E will arise.[27] Some of these additional molecular E states may be purely composed of $|i \neq 0\rangle_e$ or will at least contain significant fractions of these AO's. As only these AO's show zero order spin-orbit coupling (see the Appendix), the paramagnetic MCD properties of A_1-E transitions will be determined by them. Schematically, we may write the ground states as $|A_1\rangle = |i = 0\rangle_{a_1} + \delta_1|i \neq 0\rangle_{a_1} + \delta_2|i \neq 0\rangle_e$ and the excited states as $|E\rangle = \alpha|i \neq 0\rangle_{a_1} + \beta|i \neq 0\rangle_e + \delta_3|i = 0\rangle_e$. Here, β is assumed to be a substantial fraction, while the δ_j are small numbers of the order $\frac{h_{ij}}{\epsilon}$, as mentioned

above.

If the orbitals read like above, the strength of electric dipole transitions from $|A_1\rangle$ to $|E\rangle$ will finally be determined by matrix elements of the type $\langle i|\mathbf{r}|j\rangle$. Since the AO's are well localized, one may assume that $\langle i|\mathbf{r}|j\rangle = 0$ for $i \neq j$. In addition, taking into account the selection rules (see below) for the polarization used experimentally, we arrive at the conclusion that the transition probabilities are determined by the admixtures δ_j and β. Without a complete quantitative calculation these parameters remain unknown, but we will see that they merely account for the strength of the MCD. The shapes of the MCD bands may be predicted from the symmetry of the molecular states alone, as will be done in the following section. There, the coefficients δ_j and β will be "hidden" in reduced matrix elements, which are of secondary interest in this paper.

In summary, we conclude from the above model calculation and the subsequent argumentation that the excited states of an intervalence transfer transition from either Nb_{Li}^{4+} or Ti_{Li}^{3+} may be described as MO's based on AO's $|dt_2a_1\rangle$ and $|dt_2e\rangle$ of the central ion and the surrounding Nb_{Nb} ions. Several of these molecular states will belong to representation E, which may contribute to the MCD (see next section). The splitting between these excited states is mainly determined by exchange integrals similar to the parameter J of the simple calculation above, using $|dt_2a_1\rangle$ only. As J accounts for the interaction between Nb_{Nb} ions only, this splitting is approximately independent of the impurity ion and the excited E states may be considered as hostlike. The latter point will no longer be valid if the excited crystal field states $|dee\rangle$ (Fig. 4) of the central ion 0 have comparable energy, that is, if $10Dq \approx \epsilon$. In this case also impuritylike excited E states may result.

These findings are the basis for the interpretation of the observed MCD spectra, to be given below, because they allow us to explain, at the same time, the striking similarities at low and the pronounced differences at high energies, visible in parts (a) and (b) of Fig. 3. In order to explain this in more detail, one first has to study, which MCD band shape one has to expect for A_1-E transitions from group theory.

B. Shape of MCD bands

As already mentioned, the point symmetry of the cluster is C_{3v}. In this group, for σ light the only allowed electric dipole transition from an A_1 state is to E states, because the operators for both σ^+ and σ^- polarization transform like E. That is why emphasis was put on E-type molecular states in the above section. Taking into account the spin and the spin-orbit coupling represented by the equivalent operator $H_{s.o.} = \lambda \mathbf{LS}$, the E states split into spin orbitals E' ("1/2-like") and P_1,P_2 ("3/2-like"),[14] with energy difference $|\lambda|$. Situations in which the 3/2-like states are below the 1/2-like states are usually described by λ being negative. This case has been observed for, e.g., the first excited state of F centers in alkali halides, but also for the above-mentioned V_{Zn} in ZnSe.[23] The negative sign is also valid for $|dt_2e\rangle$ states of d^1 systems.[29] This situation is depicted in Fig. 4, where the $|dt_2ep_1,p_2\rangle$ states (3/2-like) are drawn below $|dt_2ee'\rangle$. In the excited $|dee\rangle$ spin orbitals an opposite sign has been chosen, arbitrarily. There is no first order splitting through the spin orbit coupling in these states and the actual sign of λ depend on the parameters in the Hamiltonian appropriate to the problem under consideration.[30] The question, which sign and magnitude of λ one may expect for the MO states of the Nb^{4+} cluster, will be discussed in the Appendix.

To determine the sign of λ experimentally, one first has to calculate the selection rules for transitions between the various substates of the 1/2- and 3/2-like spin orbitals by applying the Wigner-Eckart theorem (with the aid of the tables in Ref. 14). Taking also advantage of time reversal symmetry (Ref. 14, Chap. 14), we arrive at the values given in Table II. It has to be pointed out that Table II does not depend on the type of the orbital part of the states.

We keep in mind that in strong magnetic fields and at low temperatures only the spin-down state $E'\beta'$ of the ground state is populated substantially. Thus, one reads from the last row of Table II opposite MCD signs for transitions to E' and P_1, P_2 irrespective of the relative magnitude of real and imaginary parts of the reduced matrix element ρ_2. More precisely, P_1, P_2 give rise to a negative MCD band, whereas E' leads to a positive one. Consequently, the MCD spectrum connected with the excited pair of states E' and P_1, P_2 is composed of two oppositely directed bands, which lie close together, since $|\lambda|$ will be shown to be very small compared with the observed bandwidth (see below). In addition, as the spin-orbit coupling is weak, the orbital part of the states may be assumed to be either purely A_1 or E; that is, any mutual admixtures between these two orbital states via the spin-orbit coupling is neglected here (in contrast with Ref. 23).

TABLE II. Selection rules for σ^+ and σ^- transitions $E'(A_1) \rightarrow E'(E)$ and $E'(A_1) \rightarrow P_1, P_2(E)$ in group C_{3v}. ρ_1, reduced matrix element $\langle E' \parallel E \parallel E'\rangle$; ρ_2, $\langle P_1 \parallel E \parallel E'\rangle$. At low temperatures only $E'\beta'(A_1)$ is populated and a positive MCD results for $E'(A_1) \rightarrow E'(E)$ and a negative one for $E'(A_1) \rightarrow P_1, P_2(E)$.

		Excited orbital states E			
	Spin orbitals	$E'\alpha'(+\frac{1}{2})$	$E'\beta'(-\frac{1}{2})$	P_1p_1 $(+\frac{3}{2})$	P_2p_2 $(-\frac{3}{2})$
Ground	$E'\alpha'$	0	$\rho_1^2(\sigma^-)$	$(\mathrm{Re}\rho_2)^2(\sigma^+)$	$(\mathrm{Im}\rho_2)^2(\sigma^+)$
state A_1	$E'\beta'$	$\rho_1^2(\sigma^+)$	0	$(\mathrm{Im}\rho_2)^2(\sigma^-)$	$(\mathrm{Re}\rho_2)^2(\sigma^-)$

In this case, one may write the spin orbitals as products of orbital and spin function using vector coupling coefficients [see Eq. (A1) in the Appendix as an example] and calculate the spin matrix elements directly. This amounts to a further reduction of ρ_2 and one finds that $\mathrm{Im}\rho_2 = 0$ and $\mathrm{Re}\rho_2 = \rho_1$, with now $\rho_1 \propto \langle E \parallel E \parallel A_1 \rangle$. The latter reduced matrix element is only determined by the orbital part of the molecular spin orbitals. A calculation of $\langle E \parallel E \parallel A_1 \rangle$ would require one to set in the electric dipole operator and the MO's explicitly; i.e., one would have to solve the molecular problem and to determine the coefficients like δ_j and β, mentioned in the last section. However, irrespective of the size of $\langle E \parallel E \parallel A_1 \rangle$ (assumed to be unequal to zero), we find that the oppositely directed MCD bands belonging to E' and P_1, P_2 will have equal magnitude. In the sense of perturbation theory, also vibronic effects must be treated before spin-orbit coupling and, as a consequence, both bands should also show nearly the same width. Strongly overlapping MCD bands of identical shape, yet with opposite sign, are known to add to derivativelike bands (pseudo-A bands[12]). We therefore want to analyze the MCD spectra using pseudo-A bands.

C. Assignment of bands

Obviously, in the region from 1 to 2.2 eV, a derivative like structure is to be seen in the MCD of both Nb^{4+} and Ti^{3+} [Figs. 3(a) and 3(b)]. A fit, assuming one pseudo-A term composed of two opposite Gaussians, shows marked systematic deviations from the experimental data, but otherwise yields as an estimate for the separation between these two Gaussians of about 0.5 eV for both ions. This figure would correspond to $|\lambda|$ if these bands would be ascribed to final states E' and P_1, P_2. One would like to interpret these states as molecular states of the cluster, because according to the arguments given above, states of this type are nearly independent of the nature of central ion, being either Ti^{3+} or Nb^{4+}. However, 0.5 eV is not a reasonable value for λ of the corresponding MO's, as we will show in the Appendix. There we find instead that about 90 meV, i.e., the value for the free Nb ion,[29] must be regarded as an upper limit for that parameter. Now, even with such a small value, or smaller ones, for the separation between the E' and P_1,P_2 bands, one still obtains pseudo-A bands in a simulation. However, at least *two* of these pseudo-A terms are now needed to obtain a satisfactory fit of the data. We want to point out that a free fit using two pseudo-A terms does not give reliable results for $|\lambda|$, since the measured bands are not structured enough. $|\lambda|$ is therefore used as an input parameter. The curves and parameters used in the fit are sketched in Fig. 6 for the sake of clarity. From this figure and from Table II one may see that both excited E states should have a negative signed λ. Although there are simple arguments for negative contributions to the spin-orbit coupling parameters in our case (see the Appendix), one should keep in mind mind that Fig. 6 depicts only one possible way (the simplest one) to explain the data. More complicated superpositions are conceivable,

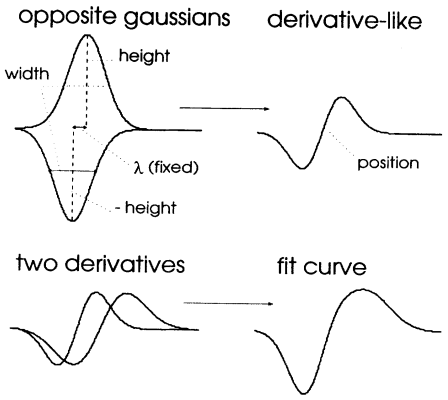

FIG. 6. Sketch of the curves used for a fit to the MCD bands. While λ is kept fixed, height, width, and position are free fit parameters for each derivative.

because a number of excited E states will be available if one increases the number of AO basis states (see the Appendix).

Table III lists the results of a fit of the data in the range 1–2.2 eV using two pseudo-A bands, each built from two opposite Gaussians with equal height and width. Here, "position" indicates the mean position of the two opposite curves and "width" is the full width at half maximum (FWHM) of a single Gaussian. No attempt has been made to use more than two pseudo-A bands in a fit, because this would be an overinterpretation of the data.

Despite the fact that the bands above 2.2 eV may influence the results, Table III reflects the similarity of the spectra of both centers below that energy. Since this resemblance is consistent with the properties of the molecular states of the cluster model, as explained at the end of Sec. IV A, we attribute both low-energy bands to intervalence transfer transitions to at least two molecular E states. Each state E is split into $\pm\frac{1}{2}$-like (E') and $\pm\frac{3}{2}$-like (P_1,P_2) states, which together yield derivativelike MCD bands. From Table III we observe that the Ti bands are somewhat shifted to higher energies. According to the cluster model, this shift simply corresponds to a lower position of the ground state for the latter ion with respect to the excited states common to both ions (see Sec. IV A).

The just given attribution of MCD bands also agrees with the fact, that the absorption is mainly σ polarized in that region [Figs. 3(α) and 3(β)]. One may wonder, however, why the obvious similarity of the MCD spectra

TABLE III. Positions and widths of pseudo-A bands in eV. The fit was to MCD spectra like those shown in Figs. 3(a) and 3(b) in the range 1–2.2 eV, which is assumed to be dominated by intervalence transfer transitions described by the cluster model.

	Position 1	Width 1	Position 2	Width 2
Nb^{4+}	1.52(1)	0.35(3)	1.73(2)	0.50(5)
Ti^{3+}	1.56(1)	0.35(3)	1.83(2)	0.55(5)

below 2.2 eV is not reflected in the σ absorption: Also in the Nb^{4+} absorption spectrum a pronounced band at 1.6 eV should be visible, the "small polaron band" known from the literature.[2] The seeming absence of this band in Fig. 3(α) results from the fact that additional diamagnetic centers, Nb_{Li}-Nb_{Nb} bipolarons,[2] are present in used $LiNbO_3$ crystals. These centers possess a wide absorption band peaked at 2.5 eV, which is superposed on the small polaron band. Illumination by light converts bipolarons to Nb_{Li}^{4+} polarons and the 1.6 eV band increases considerably by this treatment and becomes clearly visible. The relative height of the bipolaron versus the polaron band depends on the relative number of both centers, which in general is modified by the illumination process. In the case of the crystals used here, however, the number of bipolarons could not be decreased substantially. Presumably, this comes from the fact that the samples were reduced so heavily that not enough free traps were present to accommodate the electrons from the bipolarons broken by light. However, in view of the selectivity of the tagged MCD method, the presence of a strong bipolaron band is of minor importance in this work.

Again following the argumentation of Sec. IV A, one may conclude that the MCD bands above 2.2 eV, being different for both centers, are due to impuritylike excited orbitals. Good candidates for MO's at still higher energies are those which contain large fractions of the excited crystal field states $|dee\rangle$ of the central impurity ion.[31] The difference between Ti^{3+} and Nb^{4+} comes from the fact that one expects $10Dq(Ti^{3+}) < 10Dq(Nb^{4+})$.[32] Hence, the $|dee\rangle$ related bands may show up in the Ti spectrum, while they are out of range for Nb. In summary, we interpret the pronounced MCD bands above 2.2 eV of Ti^{3+} as to arise from transitions to $|dee\rangle$-like states. A corresponding band is also clearly visible in the absorption spectrum for σ polarization [Fig. 3(β)]. As for the other molecular states of symmetry E, the same arguments concerning the prediction of MCD shapes are valid here, and, of course, the data may also be represented by some superposition of pseudo-A bands. Since we are dealing with a qualitative interpretation of the spectra, however, it is not useful to actually perform such a fit.

The weak and very broad band observed above 2.2 eV in the case of Nb^{4+} [Fig. 3(a)] may either be ascribed to the low-energy wing of $|dee\rangle$-related bands, being shifted to higher energies compared to Ti^{3+}. Or it may be attributed to transitions to some other molecular states, which emerge if the orbitals $|dt_2e\rangle$ of the surrounding Nb_{Nb} are incorporated into the calculation. In this case, the corresponding band for Ti^{3+} would be hidden by the strong $|dee\rangle$-like bands existing there. In view of the very qualitative discussion of the molecular properties of the cluster, no definite attribution of this band can be given in this work.

V. SUMMARY AND CONCLUSION

Although the absorption spectra of the isoelectronic ions Nb_{Li}^{4+} ($4d^1$) and Ti_{Li}^{3+} ($3d^1$) in $LiNbO_3$ are rather weakly structured, the corresponding bands could unambiguously be correlated with these ions by the method of "tagged MCD." The attempt to assign the observed bands to specific transitions is based on the comparison of the spectra of both ions.

Above 2.2 eV, only a weak MCD signal is observed for Nb, while Ti shows rather strong bands. The bands observed for Ti are interpreted as due to transitions to delocalized molecular states with large admixtures of the Ti orbitals $|dee\rangle$. In the case of pure crystal field states (Fig. 4), the corresponding bands would yield $10Dq$ directly. From the data, we may find about 2.9 eV as an *estimate* for this parameter. It is true that this figure is within the range of 1.5–3 eV, which is found for $10Dq$ of sixfold coordinated Ti^{3+} in Ref. 33, but this may be accidental: The energy of this state should be modified by the interaction with Nb_{Nb}-like states from the conduction band, because $10Dq$ is larger than the distance of the ground state to the conduction band. In this case, the position of the MCD bands is no longer determined by the cubic crystal field alone and $10Dq$ cannot be read directly from the spectrum. Despite this complication it is clear, however, that the corresponding bands for Nb_{Li}^{4+} will be positioned at higher energies, since $10Dq$ is expected to be larger for this ion. Therefore the "$10Dq$ bands" are not found in the experimentally accessible region for this ion.

Below 2.2 eV, the MCD spectra are nearly identical for both ions. This fact suggests that the corresponding transitions lead to almost the same final states, which only weakly depend on the ion at the center of the defect, i.e., which may be called "host- or conduction-band-like." We modeled them as MO states of LCAO type. The MO's are built from orbitals located mainly on the next-nearest Nb_{Nb} neighbors, which are coupled by the superexchange interaction via oxygen ions. For states of this type and of symmetry E, the model allowed to predict derivativelike or pseudo-A shaped MCD bands. These are composed of two opposite bands of equal strength, separated by only some ten meV. Using two pseudo-A bands with these characteristics, we were able to satisfactorily fit the experimental MCD data below 2.2 eV. The fit data are nearly identical for Ti and Nb, except for the positions of the curves, which are shifted to higher energies in the case of Ti by 0.04–0.1 eV. According to the model, this shift should be ascribed to a higher energetic position of the Nb ground state level ϵ_{Nb} with respect to ϵ_{Ti}. This finding agrees well with ϵ_{Nb}-$\epsilon_{Ti} \approx$ 0.1 eV from independent experiments.[20]

The above summary shows that the basic features of the MCD spectra of the investigated d^1 ions in $LiNbO_3$ may in principle be explained by the cluster model. It remains to be seen to what extent the given arguments may be developed to explain further optical or even photorefractive properties, possibly related to Nb_{Li}^{4+}.[5]

As already mentioned in Sec. IV A, the interpretation of the low-energetic MCD bands of Nb^{4+} and Ti^{3+} in $LiNbO_3$ and that of the MCD spectrum of V_{Zn} in ZnSe (Ref. 23) have some common aspects: In both cases, the point symmetry of the defect center is C_{3v}, A_1-E transitions are inspected, and the analyses are based on MO-type orbitals. Experimentally, the MCD spectra show

a similar feature (although with different absolute sign): Two overlapping, yet well separated bands with opposite sign are observed for both centers. To ascribe this feature to a single E state, split into $\pm 3/2$- and $\pm 1/2$-like states (modified F-center case), is ruled out in both works. The final explanation of the just mentioned MCD structure is different however: Jeon *et al.*[23] found by detailed and quantitative considerations of the transition probabilities that those V_{Zn} centers are responsible for the MCD structure in question, which have their threefold axis perpendicular to the optical axis. For this orientation, A_1-A_1 transitions have to be taken into account, too, and the mentioned MCD structure is interpreted as the *sum of two absorptivelike MCD bands.* As the directions of the trigonal distortion of the V_{Zn} centers are distributed randomly in cubic ZnSe, the case of perpendicularly oriented centers necessarily occurs there. Here, with $LiNbO_3$ this situation does not apply, since the host crystal is trigonal and all Nb^{4+} centers are supposed to have approximately parallel threefold axes, which coincide with the crystal's c axis. With light perpendicular to c, the MCD cannot be measured, because the circular polarization is completely destroyed by the strong linear birefringence of $LiNbO_3$. In the present case, the mentioned MCD feature is alternatively explained as the *sum of two derivativelike bands*, belonging to two different excited E states. Also, the sign of the spin-orbit coupling constant, used to interpret the MCD, is negative in both analyses. Whereas there seems to be no simple mechanism yielding that sign in the case of V_{Zn}, negative contributions to λ are easily found in our case (see the Appendix).

Finally, it should be mentioned that the present MCD analysis, being of qualitative nature, does not allow one to decide the often discussed question, whether the central ion (Nb or Ti) is on a Nb or Li site. This is so because the symmetry of the cluster would be the same in both cases; merely the strength of the interaction between the Nb_{Nb} ions had to be modified accordingly. The consequences of these modifications may only be estimated by quantitative calculations. From the experimental side, valuable information on this question will be obtained from MCD and ODMR measurements with reduced $LiNbO_3$ crystals codoped with Mg, Zn, or In, in which presumably the free polaron Nb_{Nb}^{4+} has recently been observed optically and by EPR.[34]

ACKNOWLEDGMENTS

We thank O.F. Schirmer and M. Wöhlecke for helpful discussions, and B. Briat, ESPCI Paris, for help in confirming our MCD sign. This work was supported by the Deutsche Forschungsgemeinschaft, Sonderforschungsbereich 225.

APPENDIX

In the discussion it was stated that a value of some ten meV should be a good estimate for the upper bound of the spin-orbit (s.o.) coupling constant λ in the excited E states, to which the intervalence transfer occurs. The parameter λ has been chosen to describe the energy difference between E' ("1/2-like") and P_1,P_2 ("3/2-like") (Ref. 14) MO states resulting from s.o. coupling. Usually, λ is inferred by writing the s.o. Hamiltonian in the form $H_{s.o.} = \lambda \mathbf{LS}$, which represents an operator equivalent to a "true" one, $h_{s.o.}$ (see below). Using $H_{s.o.}$, one obtains a splitting of the size of λ between those states E' and P_1,P_2, which result from single ion orbital states $|dt_2e\rangle$ (in the chain notation for full rotation and cubic and trigonal groups, respectively[14]). Hence, sign and magnitude of λ are determined by both the proportionality constant between the equivalent operators $H_{s.o.}$ and $h_{s.o.}$ and the wave functions representing the E state. $H_{s.o.}$ is supposed to act within E states only and the resulting spin orbitals do not contain A_1 molecular orbitals, in contrast with Ref. 23. Thinking in terms of AO orbitals, this means the following: It is supposed that the molecular interactions are much stronger than the s.o. coupling, and that consequently the molecular problem may be solved first, ignoring $h_{s.o.}$. If the MO $|E\rangle$ states contain AO's of the type $|dt_2a_1\rangle$ [see Eq. (A7), below], this is not due to the s.o. coupling but rather results from the exchange coupling. This assumption may be a crude one, but it keeps the general discussion of the problem tractable.

To obtain a useful estimate for λ, as defined in the present case, i.e., for MO's, one must examine how the s.o. interaction may be evaluated using $h_{s.o.}$ and molecular orbitals $|E\rangle$. The following approach and the evaluation of "orbital reduction factors" due to covalency in EPR studies[29] make use of some common arguments, but are not identical, mainly because the covalency considered there is between metal ions and light ligand atoms, whereas we are dealing with metal ions alone.

In our model, the excited MO's are mainly built from Nb-like orbitals located on ions number 1–6 (Fig. 5). Hence, the s.o. coupling occurs in the electric fields of the corresponding niobium nuclei and the Hamiltonian $h_{s.o.}$ may be approximated by a sum of *local* s.o. operators,[35] $h_{s.o.} = \sum_i \xi(r_i)\mathbf{L}_i\mathbf{S}$. Here, the radial function $\xi(r_i)$ and the orbital angular momentum operator both depend on coordinates measured from niobium ion i. Writing $h_{s.o.}$ as a sum of local operators is justified by the observation that $\xi(r_i)$ rapidly decreases with increasing distance r_i. Quite generally, $\sum_i \xi \mathbf{L}_i$ transforms as an axial vector $\mathbf{u}$ and the scalar product with spin yields a totally symmetric operator. As a consequence, $h_{s.o.}$ *must* be diagonalized by the basis states of the half integer representations of C_{3v}. With spherical vector components one may write $h_{s.o.} = s_1 u^E_{-1} + s_0 u^{A_2}_{a_2} + s_{-1} u^E_1$.[14] Here, $s_{\pm 1} = \frac{\mp 1}{\sqrt{2}} s^{\pm}$, where $s^{\pm}$ are the usual step-up and step-down spin operators and s_0 is the z component of the spin. The u^a_α transform as the partner α of the irreducible representation a. Using the latter form of $h_{s.o.}$ and the decomposition of the "+3/2-like" state $|P_1p_1\rangle$ (arbitrarily chosen) into spin and orbital parts,[14]

$$|P_1p_1\rangle = \tfrac{-1}{\sqrt{2}}|\tfrac{1}{2}\tfrac{+1}{2}\rangle|E+1\rangle + \tfrac{i}{\sqrt{2}}|\tfrac{1}{2}\tfrac{-1}{2}\rangle|E-1\rangle, \quad \text{(A1)}$$

one finds for the s.o. energy of $|P_1 p_1\rangle$

$$E_{\text{s.o.}} = \langle P_1 p_1 | h_{\text{s.o.}} | P_1 p_1 \rangle = \tfrac{1}{2\sqrt{2}} \langle E \parallel u^{A_2} \parallel E \rangle. \quad \text{(A2)}$$

An additional part containing the reduced matrix element $\langle E \parallel u^E \parallel E \rangle$ has been dropped from (A2), since it can be shown that it would lead to a splitting of the time conjugate states $|P_1 p_1\rangle$ and $|P_2 p_2\rangle$ and consequently must vanish because of time reversal symmetry. We now define

$$\lambda = \tfrac{1}{\sqrt{2}} \langle E \parallel u^{A_2} \parallel E \rangle. \quad \text{(A3)}$$

In obtaining Eq. (A3) the matrix elements of the spin are completely evaluated and only the orbital parts of Eq. (A1), $|E \pm 1\rangle$, must be considered to obtain an estimate for the reduced matrix element $\langle E \parallel u^{A_2} \parallel E \rangle$. In the case of the usual problem, mentioned at the beginning of this appendix, concerning a single ion influenced by crystal fields, this reduced matrix element may easily be evaluated yielding the well-known[29] result $\lambda = -\langle \xi \rangle$, if $|dt_2 e\rangle$ is the orbital part in Eq. (A1). Here, $\langle \xi \rangle$ is the (positive) expectation value of the radial part of $h_{\text{s.o.}}$ for the d functions applied. In the present MO case, however, we must "unreduce"[14] $\langle E \parallel u^{A_2} \parallel E \rangle$ with $|E\rangle$ being a molecular orbital obtained from solving the cluster problem and with u^{A_2} being replaced by the true operator $\sum_i \xi L_{z_i}$. In this procedure of "unreduction" one is allowed to use an arbitrary partner state (e.g., $|E+1\rangle$) of the representation E in the matrix element. Within the basis of a doublet E found by solving the molecular problem it is always possible to form such states which transform according to $|E+1\rangle$ and $|E-1\rangle$. Supposing

$$|E+1\rangle = \sum_{i,p} c_{i,p} \varphi_i^p, \quad \text{(A4)}$$

where φ_i^p is the pth crystal-field orbital of ion i, and assuming that $\sum_i \xi L_{z_i}$ is strictly local, one has

$$\begin{aligned} \langle E \parallel u^{A_2} \parallel E \rangle &= \sqrt{2} \left\langle E+1 \left| \sum_i \xi L_{z_i} \right| E+1 \right\rangle \\ &= \sqrt{2} \langle \xi \rangle \sum_i \sum_{p,q} c_{i,p}^* c_{i,q} \langle \varphi_i^p | L_{z_i} | \varphi_i^q \rangle, \end{aligned} \quad \text{(A5)}$$

where $\langle \xi \rangle$ represents the radial expectation value for the crystal-field orbitals of Nb. Approximately, $\langle \xi \rangle$ should be the same for all φ_i^p. From (A3) and (A5) one reads

$$\lambda = \langle \xi \rangle \sum_i \sum_{p,q} c_{i,p}^* c_{i,q} \langle \varphi_i^p | L_{z_i} | \varphi_i^q \rangle, \quad \text{(A6)}$$

which gives the link between the general parameter λ and the single-ion matrix elements.

Now one has to discuss which kind of orbitals φ^p have to be considered in a realistic model. Taking into account only those of the type $|dt_{2g} a_1\rangle \propto 3z^2 - r^2$, Eq. (A6) will necessarily lead to $\lambda = 0$. This is the reason why our simple LCAO calculation can at best give an idea about the MCD bands, which would be obtained in a more realistic, but much more elaborate approach. One should use the whole cubic set of symmetry T_2, i.e., the states $|dt_2 a_1\rangle$ *and* $|dt_2 e \pm 1\rangle$, because of two reasons: First, the trigonal crystal field is possibly weaker than the exchange matrix elements h_{ij} (see Sec. IV). Second, only the incorporation of the states $|dt_2 e \pm 1\rangle$ into the MO's yields $\lambda \neq 0$.

About the magnitude and sign of λ one may now argue as follows: The AO orbitals φ^q are now from the set $|dt_2 a_1\rangle$ *and* $|dt_2 e \pm 1\rangle$ and it is not *a priori* clear which ones have to be used for Eq. (A4). Especially it must not be concluded that, e.g., $|E+1\rangle$ may only contain $|dt_2 e + 1\rangle$. For the example of a planar molecule with symmetry D_3, Table E.7.1 of Ref. 14 shows that ligand AO's transforming as $|e+1\rangle$, $|e-1\rangle$, and $|a_1\rangle$ are allowed as a symmetry-adapted MO of type $|E+1\rangle$. The second choice corresponds to a MO state having opposite local "circulation" at the ligands. An example (in cubic symmetry) of this situation is given by the excited $2p$ state of F centers in alkali halides. There, the opposite circulation results from the orthogonalization of the F center envelope function and was shown to yield a negative sign of λ.[35] The same mechanism was also considered by Jeon *et al.*[23] for V_{Zn} in ZnSe. Since we do not know the distinct composition of $|E+1\rangle$ in our case, we write most generally

$$|E+1\rangle = \sum_i \alpha_i |dt_2 e + 1\rangle + \beta_i |dt_2 e - 1\rangle + \gamma_i |dt_2 a_1\rangle. \quad \text{(A7)}$$

Using Eq. (A7) instead of Eq. (A4), Eq. (A6) becomes

$$\lambda = \langle \xi \rangle \sum_i (|\beta_i|^2 - |\alpha_i|^2). \quad \text{(A8)}$$

Here, it has been accounted for the negative effective orbital momentum[29] of the $|dt_2\rangle$ triplet, that is $\langle dt_2 e \pm 1 | L_z | dt_2 e \pm 1 \rangle = \mp 1$. It follows from Eq. (A8) that (i) $|\lambda| < \langle \xi \rangle$, since $|E+1\rangle$ [Eq. (A7)] is assumed to be normalized and the γ_i do not contribute. Furthermore, the contributions from α_i and β_i will cancel to a certain amount. (ii) The sign of λ depends on the precise values of the α_i and β_i, being negative for $|\alpha_i|^2 > |\beta_i|^2$. The latter condition means that the ligand AO's have predominantly the same sense of circulation as the MO-type total state. There seems to be no argument against this choice, which directly leads to negative contributions to λ. The same situation results in a positive sign, however, if p-type ligand orbitals are involved, as is the case for V_{Zn} in ZnSe.[23]

[1] A. Räuber, in *Current Topics in Materials Science*, edited by E. Kaldis (North-Holland, Amsterdam, 1978), Vol. 1.
[2] O.F. Schirmer, O. Thiemann, and M. Wöhlecke, J. Phys. Chem. Solids **52**, 185 (1991).
[3] B. Dischler, J.R. Herrington, A. Räuber, and H. Kurz, Solid State Commun. **14**, 1233 (1974).
[4] A. García-Cabañes and J.M. Cabrera, J. Phys. Condens. Matter **5**, 2267 (1993).
[5] F. Jermann and J. Otten, J. Opt. Soc. Am. B **10**, 2085 (1993).
[6] L. Arizmendi, J.M. Cabrera, and F. Agulló-López, J. Phys. C **17**, 515 (1984).
[7] O.F. Schirmer and D. von der Linde, Appl. Phys. Lett. **33**, 35 (1978).
[8] J.L. Ketchum, K.L Sweeney, L.E. Halliburton, and A.F. Armington, Phys. Lett. **94A**, 450 (1983).
[9] O.F. Schirmer, S. Juppe, and J. Koppitz, Cryst. Lattice Defects and Amorph. Mater. **16**, 353 (1987).
[10] D.A. Dutt and G.G. DeLeo, J. Phys. Chem. Solids **51**, 407 (1990).
[11] Whenever the site of the ions becomes clear from the context, we will omit the subscript "Li" from the symbols in the following.
[12] P.J. Stephens, in *Advances in Chemical Physics*, edited by I. Prigogine and Stuart A. Rice (Wiley, New York, 1976), Vol. 35.
[13] B. Briat, in *Electronic States of Inorganic Compounds: New Experimental Techniques*, edited by P. Day (Reidel, Dordrecht, 1975).
[14] S.B. Piepho and P.N. Schatz, *Group Theory in Spectroscopy* (Wiley, New York, 1983).
[15] J.-M. Spaeth and F. Lohse, J. Phys. Chem. Solids **51**, 861 (1990).
[16] P.G. Baranov (unpublished).
[17] B. Briat, C. Laulan Boudy, and J.C. Launy, Ferroelectrics, **125**, 467 (1992); B. Briat (unpublished).
[18] H. Müller and O.F. Schirmer, Ferroelectrics **125**, 319 (1992).
[19] The positions within the line, B_{low} and B_{high}, are shown in Fig. 2, although this is an ODMR spectrum at 70 GHz.
[20] O. Thiemann, H. Donnerberg, M. Wöhlecke, and O.F. Schirmer, Phys. Rev. B **49**, 5845 (1994).
[21] P. Nagels, in *The Hall Effect and its Applications*, edited by C.I. Chien and C.R. Westlake (Plenum, New York, 1980).
[22] U. Kaufmann and J. Windscheif, Phys. Rev. B **38**, 10060 (1988).
[23] D.Y. Jeon, H.P. Gislason, and G.D. Watkins, Phys. Rev. B **48**, 7872 (1993).
[24] H. Donnerberg, S.M. Tomlinson, C.R.A. Catlow, and O.F. Schirmer, Phys. Rev. B **44**, 4877 (1991).
[25] C. Zaldo, C. Prieto, H. Dexpert, and P. Fessler, J. Phys. Condens. Matter **3**, 4135 (1991).
[26] W.A. Harrison, *Electronic Structure and the Properties of Solids* (Freeman, San Francisco, 1980).
[27] M. Tinkham, *Group Theory and Quantum Mechanics* (McGraw-Hill, London, 1964).
[28] I.G. Austin and N.F. Mott, Adv. Phys. **18**, 51 (1969).
[29] A. Abragam and B. Bleaney, *Electron Paramagnetic Resonance of Transition Ions* (Clarendon, Oxford, 1970).
[30] R.M. Macfarlane, J.Y. Wong, and M.D. Sturge, Phys. Rev. **166**, 250 (1968).
[31] We continue to call these states "molecular," because their energetic position is within the conduction band and they should consequently show distinct $\mathrm{Nb}_{\mathrm{Nb}}$ character. If the cubic crystal-field parameter $10Dq$ would be less than the distance of the ground state to the conduction band ϵ, the corresponding excited molecular state would reduce to the "ordinary," well-localized crystal-field state $|dee\rangle$. We investigated Al_2O_3:Ti as an example for such a system.
[32] S. Sugano, Y. Tanabe, and H. Kamimura, *Multiplets of Transition Metal Ions in Crystals* (Academic, New York, 1970).
[33] A.B.P. Lever, *Inorganic Electronic Spectroscopy* (Elsevier, Amsterdam, 1984).
[34] B. Faust, H. Müller, and O.F. Schirmer, Ferroelectrics (unpublished).
[35] D.Y. Smith, Phys. Rev. B **6**, 565 (1972).

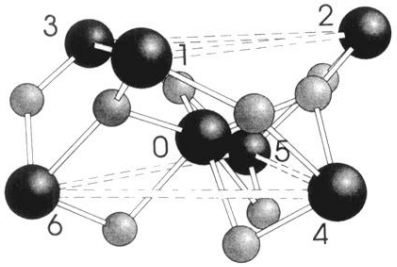

FIG. 5. Fragment of $LiNbO_3$ consisting of a central ion 0 (Ti^{3+} or Nb^{4+}) on a Li site and the next-nearest Nb_{Nb} ions (1–6). The oxygen ions forming bonds between the cations are shown with a lighter texture. The dashed sticks have been added to illustrate the trianglelike symmetry of the cluster. If ion 0 is ignored, ions 1–6 form a molecule, which has similar symmetry properties as benzene.